Digital Manufacturing Technology
https://ojs.wiserpub.com/index.php/DMT/

UNIVERSAL WISER PUBLISHER

Research Article

Stiffness Degradation of PolyJet Printed Nano Embedded Configuration with Digital Material

Ravi Pratap Singh Tomar, Furkan Ulu, Ram V. Mohan*, Ajit D. Kelkar

North Carolina A&T State University Greensboro, NC/USA 27411
E-mail: rvmohan@ncat.edu

Received: 1 November 2022; **Revised:** 20 December 2022; **Accepted:** 4 January 2023

Abstract: Introduction: Polymer-based additive manufacturing (AM) parts are used in a variety of engineering applications in the automotive, aerospace, and energy industries. However, AM printed parts are a new class of materials and the structural performance of these materials is not yet fully understood, and research on the exact performance of PolyJet printed parts and related digital materials under fatigue loading is still minimal. The present study provides insight into the fatigue damage state, cyclic performance, and comparison between pristine (baseline) and Carbon Nano Fibers (CNFs) modified embedded test coupons formed using tailored digital designs and printed with digital polypropylene from PolyJet printing. **Methods:** The investigations employed 3-dimensional (3D) test coupons formed using PolyJet printing. The nanomodified coupons were formed using digital design configurations for tailored deposition locations that allowed the integration in a 2-step process. The limitations of the conventional ASTM D638 2-dimensional (2D) test coupon for AM-treated materials caused by the process are eliminated by the homogeneous 3D test coupon used in this work. An analytical model of the accumulated damage state based on stiffness deterioration under cyclic loading is presented along with an empirical model of effective elastic modulus based on the analysis of fatigue data. Additionally, the predicted model and the actual damage accumulation due to cyclic loading are compared. **Results:** With a high correlation coefficient, R^2 of 0.9971 for the baseline and 0.9885 for the CNFs embedded configuration, it is observed that the linear function model can estimate fatigue life with an agreement to experimental results and can be used to extrapolate for other stress levels. CNFs modified resin embedded configuration showed lower fatigue life as compared to baseline. This reduction can be attributed to the stress concentration at the interfaces. **Conclusion:** This work fills the gap in the literature by characterizing the fatigue life, and cyclic performance of PolyJet printed parts and nano-modified systems with digital material.

***Keywords*:** additive manufacturing, fatigue life, analytical modeling

1. Introduction

Due to the freedom in design flexibility and customized modification over the morphology of final parts by adding necessary materials layer by layer, polymer-based additive manufacturing (AM) parts have become more and more popular in a variety of engineering applications including automotive, aerospace, and medical devices [1-4]. Some of these applications involve fatigue loading, which involves subjecting the materials to cyclic loads below their ultimate tensile strength (UTS) [5, 6]. The development of microcracks as a result of these repetitive cyclic stresses leads to the deterioration of mechanical characteristics and failure from fatigue loading. Therefore, it is crucial to comprehend how

DOI: http://doi.org/10.37256/dmt.3120232122

these structural components behave under fatigue and to create models that can anticipate how much fatigue damage would accumulate over time in the material [7, 8]. The fatigue behavior of polymers is generally studied via extensive experiments and empirical models for fatigue life or damage from experimental data. For calculating fatigue damage accumulation, a variety of approaches have been established based on various damage measures. The studies aim to establish a method to predict fatigue damage by conducting a minimum of experiments. The stiffness/strength-based model captured the gradual degradation of the sample in terms of its stiffness or strength. The stiffness-based model results change in the stiffness of material undergoing fatigue. The residual stiffness is obtained from the initial stiffness of the material and the applied number of cycles. These three parameters can be expressed in mathematical model forms such as linear, power, or sigmoidal, depending on the experimental data. Similarly, a strength-based model is developed using residual strength as a damage parameter. Estimating residual strength and fatigue life requires destructive testing, while stiffness can be evaluated nondestructively [9].

AM-printed parts via PolyJet printing have the potential to eliminate challenges in conventional manufacturing and form a newer class of digital polymeric materials [10-13]. However, relatively little research is being done currently to understand the fatigue and fracture behavior of these materials, and the structural performance of these materials is not fully understood. AM has a strong future for forming a new class of nanocomposites. Due to its ability to print intricate 3-dimensional (3D) objects layer by layer and access the part's interior volume regions during building, AM with integrated nanomaterials can be advantageous in controlling the material distribution and properties over the part volume. Embedding nanomaterials can further expand the capabilities and build via AM from the digital designs customized to specific needs. These include properties such as tailored gradient in thermal [11] and electrical conductivity and increased strength with reduced weight [14].

Most of the studies in the literature on the fatigue characterization of 3D printed materials are primarily based on ASTM D638 standard 2-dimensional (2D) test coupons. In a traditional 2D test coupon, one dimension is thinner than the other two, which could not be sufficient to account for irregularities in a material deposition during PolyJet printing. Additionally, the impact of normal strain—a compressive strain in thinner directions—is not fully understood. We have considered and assessed a homogenized 3D configuration test coupon to effectively capture the usual strain impact and comprehend the process-induced changes. A homogeneous 3D configuration is designed to keep the same cross-section's aspect ratio, as shown in Section 3.1 which allows for uniform material deposition during printing and reduces the process-induced artifacts. The objective of the 3D test configuration was to capture the processing effects without artifacts potentially resulting from different aspect ratios of the cross-sectional dimension.

Over the past years, few researchers studied developing multi-materials or functionally graded structures in AM through optimum design methods. This work considered integrating nanomaterials in PolyJet printing to develop a multi-materials system and studied their fatigue characteristics performance. Furthermore, studies on fatigue are essential due to the feasibility of integrating nanomaterials in PolyJet printing and fostering the development of new digitally tunable polymeric material structures via PolyJet printing [15, 16].

This paper compares the stiffness degradation of a pristine (baseline) and nano-modified material system under tension-tension fatigue loading of digital polypropylene (PP) using a homogenous 3D test coupon configuration built from tailored digital designs of the geometry and material distributions. The goal of this work is to gain important insight into fatigue damage state and cyclic performance of nano-modified materials system printed via PolyJet and eliminate the process-induced artifacts by implementing custom 3D test configuration.

There is some research on the fatigue properties of PolyJet printed parts, but the literature is scarce. Few research studies have been performed to develop optimal functionally graded materials with effective materials properties and desired performance in 3D printing. Doubrovski [17] used voxel-based representation to define microstructure, and Kawasaki and Watanabe [18] used the spatial distribution of materials within the specified volume. Moore and Williams [19, 20] studied the fatigue characteristics of a single elastomeric material, TangoBlackPlus (TP) at the interface printed with material jetting. They have examined the effect of no interface, single interface, and dual interface on fatigue life. Kaweesa et al. studied the fatigue life of functionally graded materials via material jetting [21]. They investigate the effects of different materials' transitions on the fatigue life of materials jetted samples. Suresh et al. investigated the fatigue life of Veroclear materials printed by PolyJet in two different build orientations and observed higher fatigue strength in perpendicular-oriented samples [22]. In fact, there is minimal existing research in identifying the fatigue properties of PolyJet parts in general. The majority of research has examined the effects of variables on the mechanical

properties of material jetted parts, including orientation, surface polish, part spacing, material anisotropy, and ultraviolet (UV) exposure [23-26].

Following a review of the PolyJet literature, it was found that no prior literature existed on the fatigue life of nano-embedded systems formed using digital design considering the 3D test coupons via PolyJet printing. To address this gap in the literature, this work fabricated the nano-materials embedded resin test coupon with tailor materials deposition and performed the fatigue characteristic with comparison to the baseline system.

2. Materials and methods

2.1 *Materials and PolyJet system*

The Stratasys J750 printer, which uses PolyJet printing technology, is used to print test specimens. VeroPureWhite (VW) and TP, which have drastically different mechanical properties at room temperature, were chosen as base materials for this study. VW is rigid at room temperature, and TP is rubbery at room temperature. Stratasys J750 can mix two base materials to form a different possible combination of digital materials that can be used to mimic natural and biological structures [27]. Figure 1 shows the two selected base materials, i.e., VW and TP, and all possible combinations. There are eight possible combinations of them depending on a specific concentration. For this work, RGD8530 is identified as a material of interest. RGD8530 is a simulated PP. Simulated PP is formed by mixing two photopolymers locally and is expected to have properties similar to homogenized standard PP polymer.

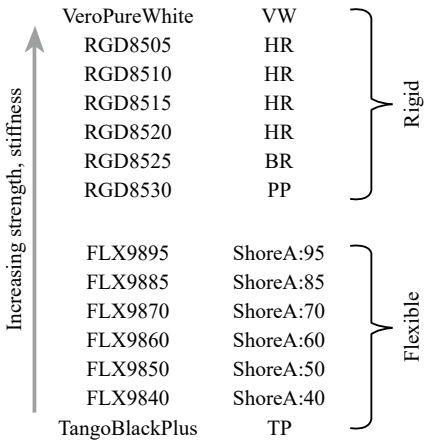

Figure 1. Different digital materials are printable from two base materials (TP and VW) with Stratasys J750 (RDG8530 is simulated PP)

2.2 *Design and fabrication of the test sample*

2.2.1 *Custom computer-aided design (CAD) of homogenized 3D tensile test coupon*

The concept behind this customized design is to keep the same cross-section aspect ratio in gauge length for uniform material deposition during printing in any build orientation. Literature has not considered such 3D specimen configurations that eliminate the geometry effects during the build process [28]. The same aspect ratio of the cross-section is maintained by using a homogeneous 3D test coupon configuration, as shown in Figure 2(b) allowing for uniform material deposition during digital design-based layer-by-layer printing and reducing the process-induced artifacts.

The traditional 2D test coupon cross-section dimensions are defined by ASTM D638 as 13 x 3.2 mm. For the custom 3D test coupons, the cross-section dimensions are designed 13 x 13 mm to keep the same cross-section aspect ratio, as shown in Figure 2(c-d).

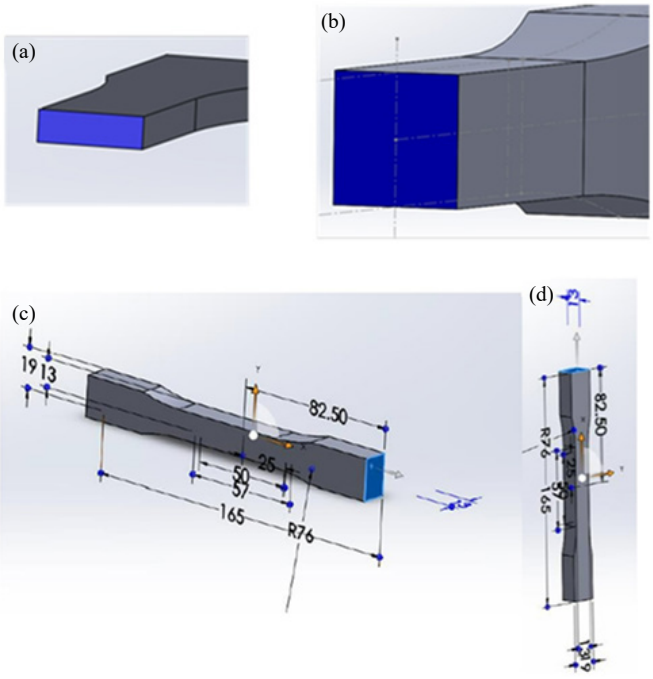

Figure 2. Cross-section: (a) Traditional 2D test coupon; (b) Homogenized 3D test coupon; (c-d) CAD design of 3D tensile test coupon

2.2.2 *Fabrication of custom 3D specimen (pristine/baseline)*

A modified configuration of 3D test coupons is employed to investigate the fatigue characterization of digitally simulated PP with test coupons formed using PolyJet printing. Tension-tension fatigue (cyclic loading) characteristic was studied by considering two build orientations that showed higher static mechanical properties. The optimum build orientation was XY print orientation. When a part is oriented, it has its longest direction along the x-axis and its second-longest direction along the y-axis. This is known as an XY-part, as shown in Figure 3. This optimal build orientation was selected for further detailed analysis, investigations of obtained fatigue data, and development of fatigue life and damage constitutive models.

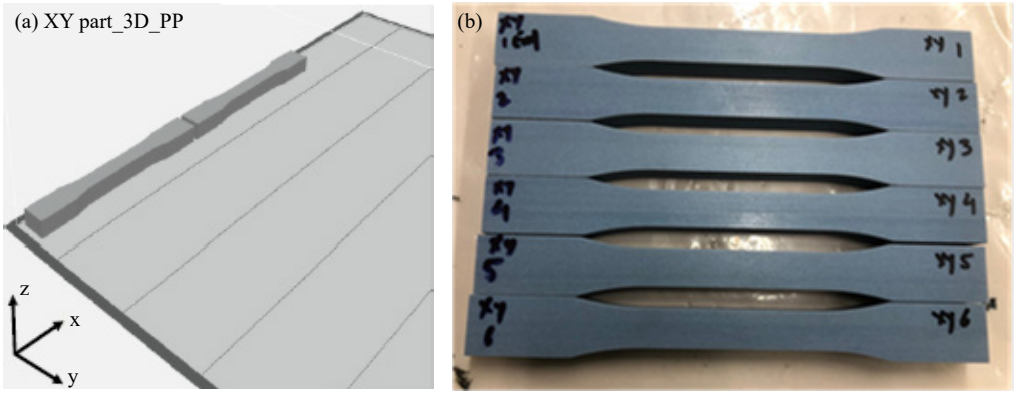

Figure 3. (a) Orienting the digital CAD design in XY orientation; (b) Test coupons printed in XY orientation (baseline)

2.2.3 *Fabrication of nanomodified 3D specimen (Carbon Nano Fibers modified resin embedded test coupons)*

The optimum build orientation XY orientation is further selected to integrate nanomaterial in the specimen. Currently, PolyJet printing technology cannot add nanoparticles during printing due to its complexity and chances of nozzle clogging in the case of nanoparticle agglomeration. Therefore, an alternative approach to introduce nanomaterials in the PolyJet system is the innovative two-step process that recently demonstrated success in our research group within PolyJet AM [29].

In the two-step digital design process of printing nanomodified material coupons, the 3D CAD model is designed with open regions where nanomaterial (carbon nanofibers) modified resin is to be placed. These regions were filled with the Carbon Nano Fiber (CNF) modified digital PP externally during the PolyJet AM process as the part was being built. The nanomodified resin integration was completed by pausing the printing, externally adding the CNF modified resin, and using an external UV light source for the polymer consolidation. The printing process was then continued to completion. The voids are designed to be selected within the gauge length of 3D tensile specimens as the gauge section deforms and failure is localized in this region, as shown in Figure 4. The dimension of these voids in the present work is selected so that it can be accessible to fill the modified resin; therefore, the dimension of voids is currently set to be in a square of 2 x 2 mm.

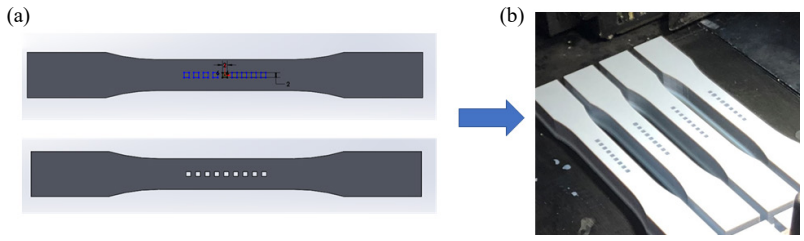

Figure 4. (a) CAD design of CNFs embedded component test coupon; (b) CNFs embedded test coupons

From the manufacturing point of view, PolyJet printing is an ink-jetting technology that deposits single drops to form a layer and cure it. To replicate the similar technology principle and optimal processing, process studies concluded that depositing a single drop of nano-modified resin in a void region followed by curing a single deposited drop was effective. The synthesis process for CNF-modified resin is schematically illustrated in Figure 5.

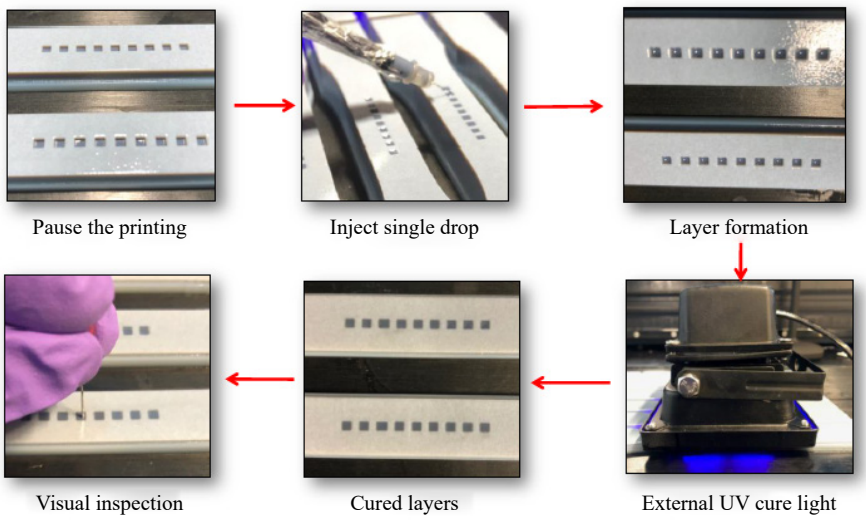

Figure 5. Synthesis process for filling the void with CNF modified resin

2.3 *Static tensile characterization*

Static tensile characterization was performed to obtain the UTS of baseline and CNF modified resin-embedded test coupons following ASTM D638 standard. Five samples were tested in each category.

2.4 *Tension-tension fatigue characterization*

The constant amplitude load-controlled tension-tension fatigue characterization of the baseline and CNF-resin modified test coupons were conducted following the ASTM D7791-17 standards. At least five samples were tested for each category. The applied load to the specimen was calculated depending on the stress level. Using a low frequency of 1 Hz, the minimum cyclic load in each case was 1/10 of the maximum load (stress ratio, S = 0.1). As a percent of the UTS, fatigue loads were applied. Fatigue tests were performed in 10% increments from 50% of UTS to 80 % of UTS. The fatigue test was stopped at the run-out value of 50,000 cycles.

3. Results and discussion

3.1 *Modeling of S-N curve*

During the product's lifecycle, it is necessary to predict the repair and replacement cycle for various components of the product. A better estimation of fatigue life is provided using S-N diagram modeling. By performing regression analysis on experimental data and selecting the best-fit model to predict the fatigue life under tension-tension fatigue loading, fatigue life modeling of AM printed test coupons is conducted.

Linear regression analysis can best represent the trend of fatigue data. Linear regression was to predict the fatigue life of homogenized 3D test coupons for baseline and CNF-resin embedded test coupons. The equation of a line used is shown in equation (1):

$$Y = ax + b, \tag{1}$$

where $Y = S/S_u$ and $x = \text{Log N}$.

The estimated values of the parameters a and b for the S-N diagram of 3D test coupons for baseline and CNF-resin embedded coupons are shown in Table 1.

Table 1. Parameter values for linear regression

Parameter	Baseline	CNFs embedded
a	1.5039	1.1633
b	-0.2438	-0.1697

Figure 6 shows the linear regression analysis for baseline and CNFs modified resin embedded test coupons, respectively. It is indicated that linear regression is the best-fit choice for the curve fitting of the experimental data. The high correlation coefficient, R^2 (0.9971 and 0.9885) further validates this hypothesis.

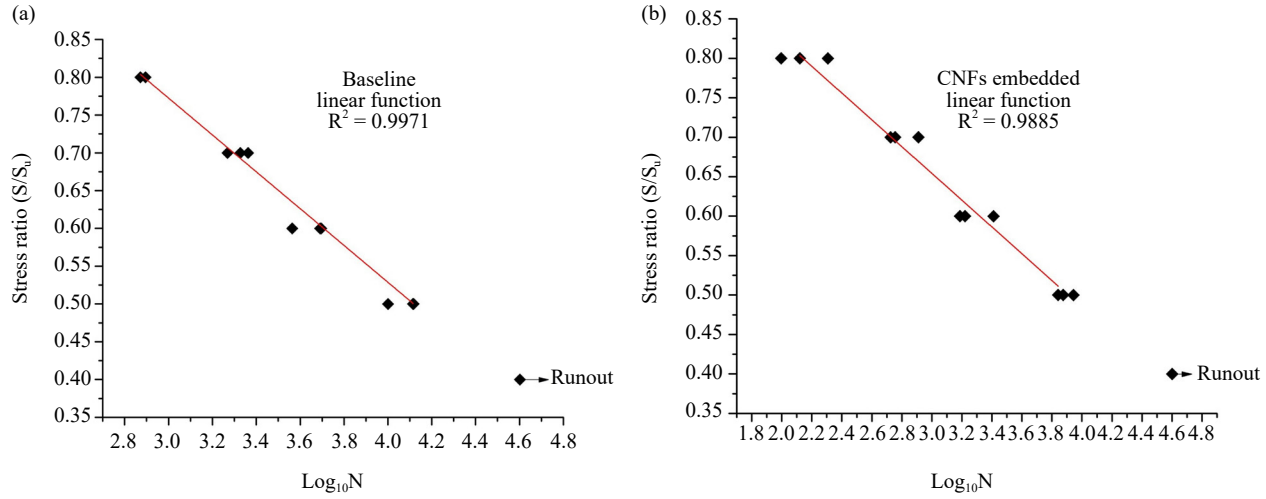

Figure 6. Representation of the S-N diagram of the test coupon: (a) Baseline; (b) CNF-resin embedded

A comparison of linear model results for baseline and CNF-resin embedded test coupons with experimental results is presented in Table 2. It is observed that the linear function model can estimate fatigue life with an agreement to experimental results and can be used to extrapolate for other stress levels.

Table 2. Comparison of a linear model with experimental results

Material system	Stress level	The average number of cycles at failure	
		Experimental	Linear
Baseline	70%	2097	1983
Baseline	80%	759	771
CNF-resin embedded	60%	1925	2086
CNF-resin embedded	70%	638	537

3.2 *Stiffness degradation*

Monitoring the fatigue damage and accumulation in AM parts is essential to understanding their structural life. Strength and stiffness are two basic properties that define the life of the AM structure. While residual strength evaluation requires destructive testing, stiffness can be evaluated nondestructively [30]. In this work, the elastic modulus is used as the parameter for investigating fatigue damage.

3.2.1 *Computation of elastic modulus*

Elastic modulus, E is computed using the fundamental relation given by the equation,

$$E = \frac{\sigma}{\varepsilon}, \tag{2}$$

where,
σ = applied stress,
ε = resulting strain.

In equation (2), stress and strain are calculated as:
Stress in tension is given by,

$$\sigma = \frac{P}{A},$$

where,
P = tensile force or load,
A = cross-section area, BL.
Strain in tension is given by,

$$\varepsilon = \frac{\Delta L}{L},$$

where,
ΔL = change in original length,
L = original length.
Replacing the term in equation (2) gives,

$$E = \frac{PL}{\Delta L.BL}. \tag{3}$$

Since the fatigue test conducted in this work is load controlled test, load, P, in the above equation is constant, whereas L, B, is the geometry constant of the test coupon. Thus, elastic modulus, E is a function of change in length, ΔL:

$$E \propto \frac{1}{\Delta L}.$$

3.2.2 *Experimental characterization of stiffness degradation*

While testing, load-displacement data is collected at peaks and valleys with the software's cyclic peak/valley data acquisition feature. The stiffness was computed by dividing the life cycle into ten segments, with the last segment further divided into five sub-segments. At the beginning and end of each segment, load-displacement reading is captured. Elastic stiffness, E, is computed at peak loads and the end of each segment using Equation (3). The computation of elastic modulus for the fatigue cycle is shown in Table 3.

Table 3. Computation of elastic modulus, E

Cycle count, N	Load, P (lb)	Change in length, ΔL (in)	Stress, σ (psi)	Strain, ε	Elastic modulus, E (GPa)	Cycle ratio (N/N_F)	Normalized modulus ($E_n = E/E_0$)
1	665.17	0.06968	2819.714	0.0178	1.076	0.0004	1.000
230	736.79	0.02362	3123.335	0.0239	0.899	0.0996	1.000
460	734.33	0.0324	3112.919	0.0261	0.818	0.1993	0.998
690	733.73	0.0396	3110.365	0.0280	0.764	0.2989	0.994
920	731.35	0.0460	3100.26	0.0296	0.719	0.3986	0.991
1150	730.94	0.0524	3098.55	0.0313	0.681	0.4982	0.989
1380	730.04	0.0588	3094.70	0.0329	0.647	0.5979	0.985
1610	729.45	0.0650	3092.20	0.0345	0.616	0.6975	0.982
1840	726.26	0.0713	3078.71	0.0361	0.586	0.7972	0.983
2070	727.21	0.0778	3082.74	0.0378	0.561	0.8968	0.975
2117	724.47	0.0791	3071.11	0.0381	0.554	0.9172	0.975
2164	722.75	0.0804	3063.82	0.0384	0.548	0.9376	0.976
2211	720.78	0.0817	3055. 46	0.0388	0.542	0.9579	0.979
2258	721.28	0.0830	3057.58	0.0391	0.538	0.9783	0.979
2305	722.78	0.0844	3063.96	0.0395	0.534	0.9987	0.975

The stiffness degradation $E_n = E/E_0$ measurement was used to assess the degree of damage in each configuration. E_0 represents the material's initial dynamic stiffness as measured in the first cycle (N=1), and E represents the stiffness of the material after n cycles. The ratio of the material's equivalent stress to strain throughout each cycle of fatigue loading is known as stiffness. This computed stiffness is plotted against the number of cycles (N) or cycle ratio (N/N_F). Here, N_F is the number of cycles at failure. The stiffness degradation of baseline and modified CNF resin-embedded test coupons at an applied stress level of 50%, 60%, and 70% of UTS, respectively, are shown in Figure 7.

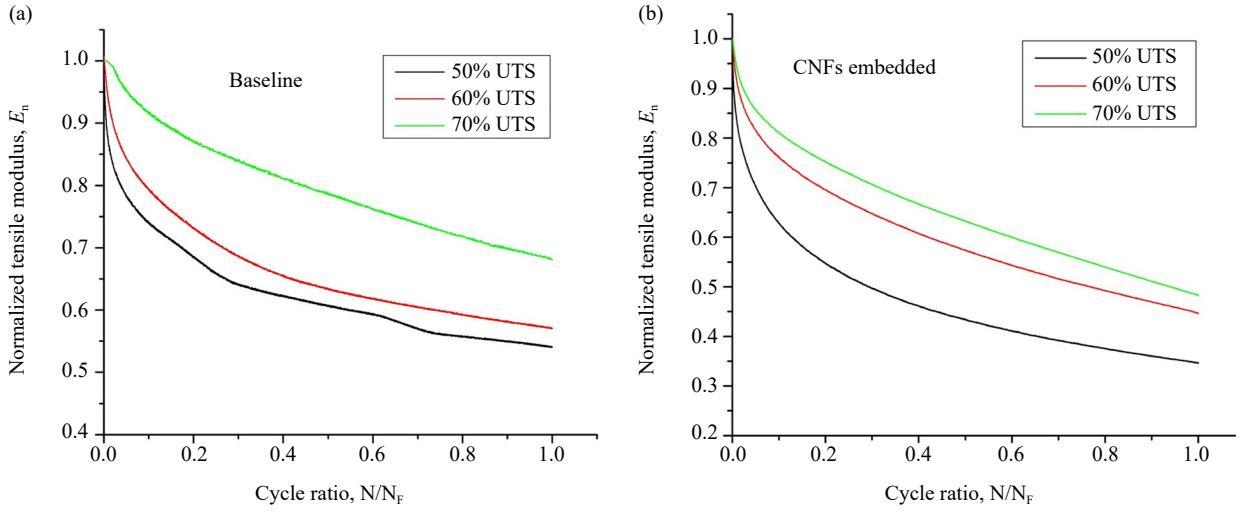

Figure 7. Stiffness degradation of test coupons at applied stress of 50%, 60%, and 70%: (a) Baseline; (b) CNF-resin embedded

Usually, a higher loading percentage in composite materials accounted for maximum stiffness degradation. In the initial stage, the matrix cracks, and in the second stage, most of the load was taken by fibers [31]. The AM printed parts of baseline, and CNF-resin embedded test coupon show the reverse trend of stiffness degradation compared to composite materials, as shown in Figure 7. This behavior can be attributed to strain hardening, where the material becomes stiffer as we apply a higher load in a polymer. So, the modulus improves due to strain hardening, but the fatigue cycle degrades the modulus. Therefore, the rate at which it degrades will be slower at lower load levels. As a result, strain hardening hardens the polymer during fatigue of AM parts under higher loading, causing less stiffness loss than lower loading.

Further, the computed stiffness for baseline and CNFs embedded test coupons for each applied stress level of 50%, 60%, and 70% of UTS are presented in Figure 8. The fatigue characterization results show that the average life of the modified CNF resin-embedded test coupons is lower than the baseline test coupons. The lower fatigue life can be attributed to CNF inclusion initiating stress or strain concentration that frequently degrades the mechanical properties. CNFs are stiffer than the polymer, and the nano-modified resin shows brittle characteristics.

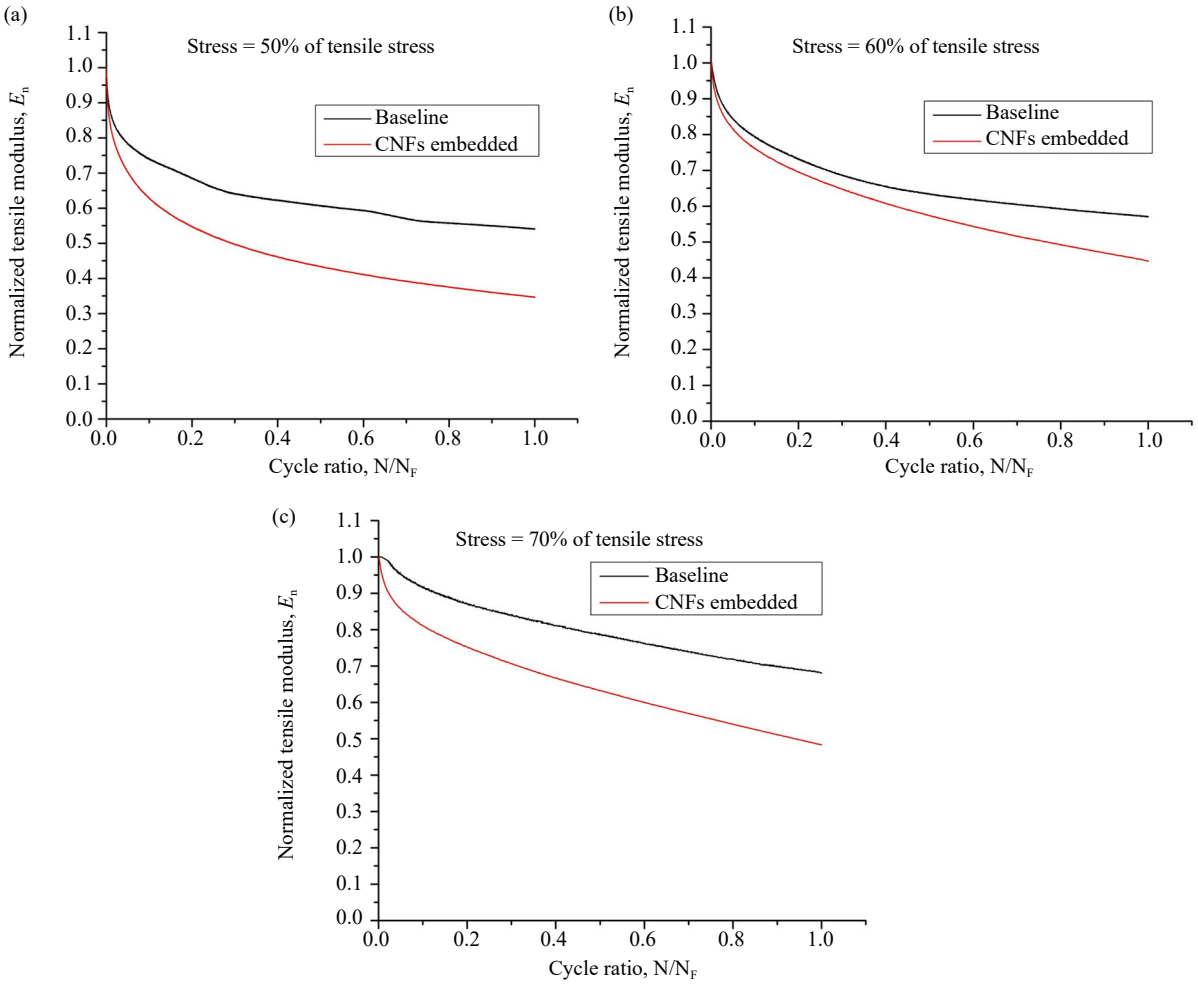

Figure 8. Comparison of stiffness degradation of baseline and CNF resin embedded at three stress levels: (a) 50%; (b) 60%; (c) 70%

3.3 *Stiffness degradation model during fatigue life*

In the stiffness degradation model, fatigue failure is expected to occur at the point when stiffness or modulus degrades to a certain threshold level. Various functions can be used to estimate stiffness degradation [5].

The stiffness degradation model considered in this work assumes a fourth-order polynomial during the fatigue

life cycle. Regression analysis of experimental data on stiffness deterioration at various percentage loading is used to construct the analytical model for stiffness degradation. A second regression analysis was performed to estimate the polynomial coefficients using the test data results at each load percentage. Then, a master curve was obtained for each coefficient that forms a degree 4 polynomial. The coefficient from the master curve can be used to model the simulated stiffness degradation for each percentage of loading and can be used to extrapolate for other loading levels [32]. The procedure for modeling stiffness degradation is outlined in Figure 9.

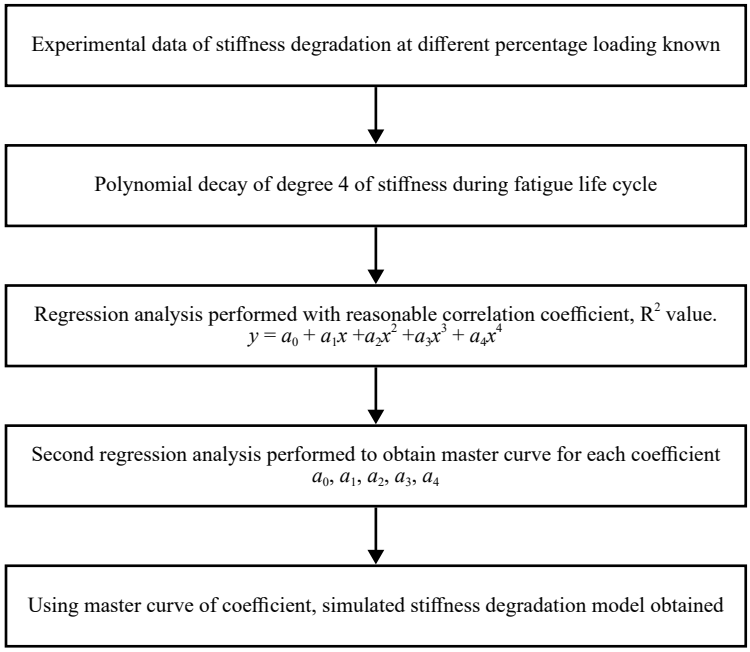

Figure 9. Methodology for modeling of stiffness degradation

Figure 10(a-c) compares the baseline experimental and simulated curves of the stiffness degradation at a stress level of 50%, 60%, and 70% of the UTS, respectively. Hence, the simulated and experimental stiffness degradation curves exhibited strong agreement.

From the master curve of the coefficients, stiffness degradation behavior was simulated at 65% loading to validate the master curve of the coefficient for baseline configuration. Figure 10(d) shows that simulated stiffness degradation at 65% was clearly between experimental data of stiffness degradation at 60% and 70 % stress levels, which validates the performed regression analysis for baseline test coupons.

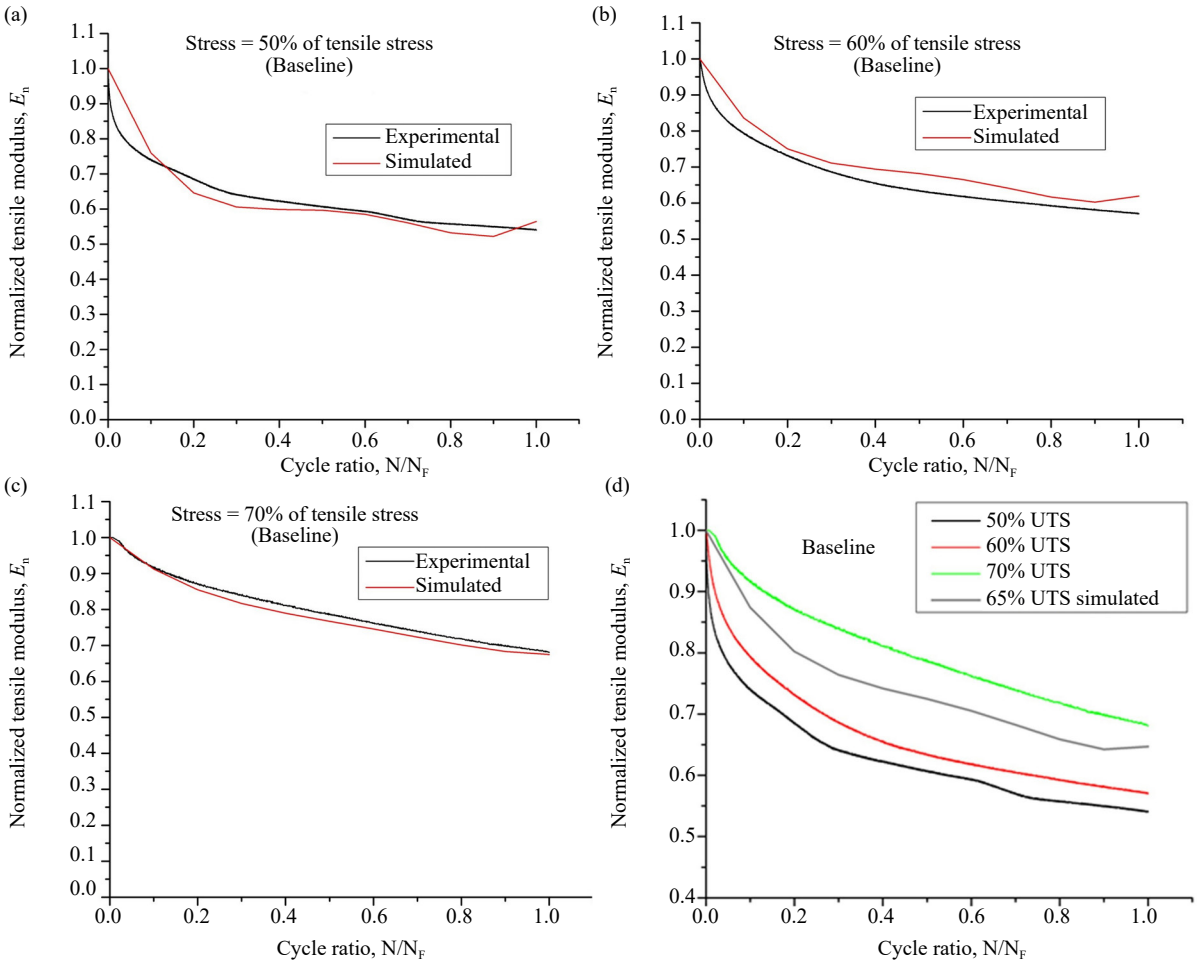

Figure 10. Comparison of baseline stiffness degradation experimental and simulated at an applied stress: (a) 50%; (b) 60%; (c) 70%; (d) simulated stiffness degradation at 65%

Further, for the CNF-resin modified test coupons, Figures 11(a-c), compare the experimental and simulated curves of the stiffness degradation at a stress level of 50%, 60%, and 70% of the UTS, respectively. As a result, the simulated and measured stiffness degradation curves showed excellent agreement.

Similarly, the master curve of the coefficient was validated for CNFs embedded configuration. Stiffness degradation was simulated at an applied stress of 55% of UTS to validate the coefficient of the master curve. From Figure 11(d), it was observed that the simulated stiffness degradation at stress level 55% of UTS was precisely in between experimental data of stiffness degradation at applied stress 60% and 70% of UTS, which validates the regression analysis for CNFs embedded test coupons.

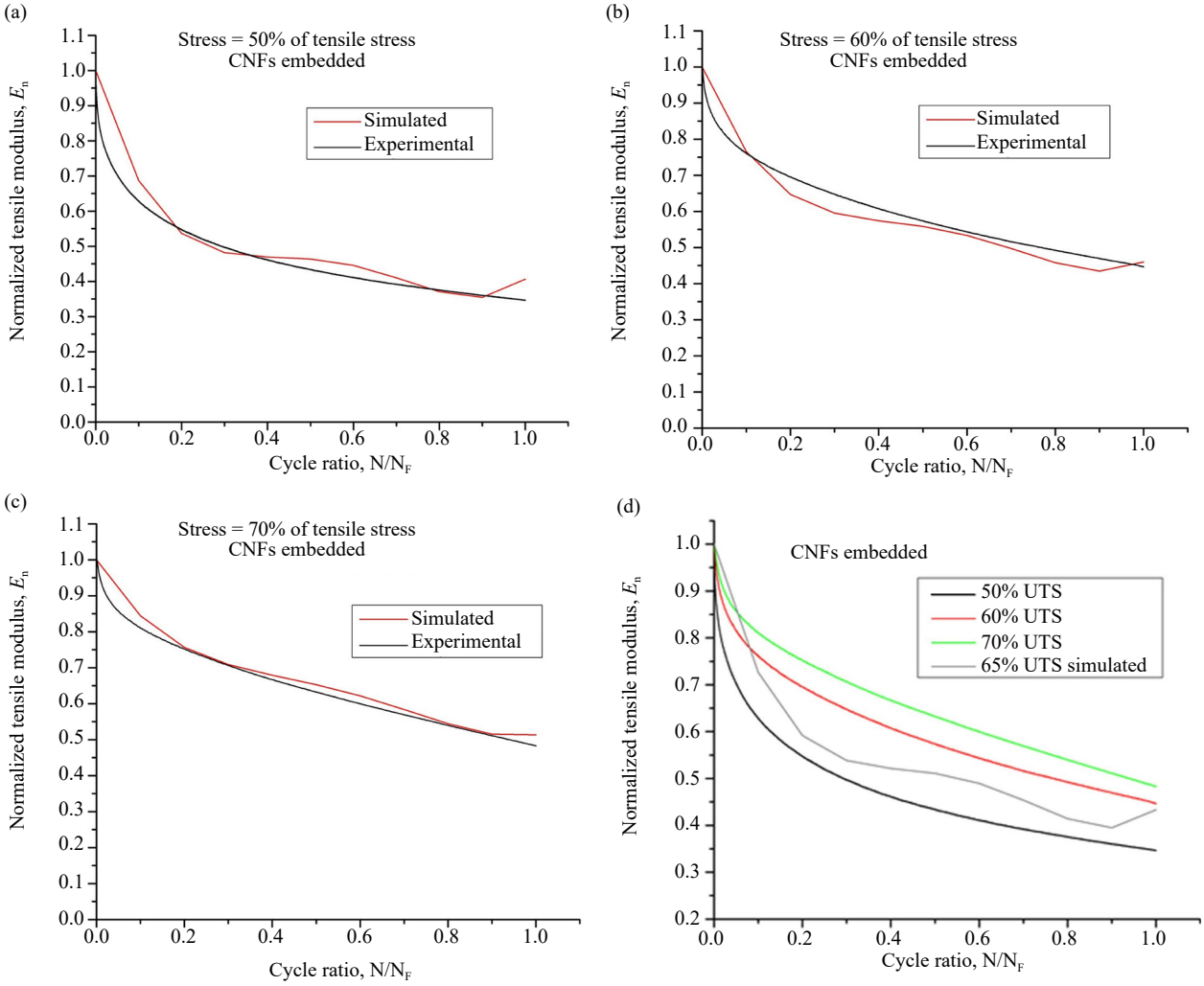

Figure 11. Comparison of CNF-resin modified stiffness degradation experimental and simulated at an applied stress: (a) 50%; (b) 60%; (c) 70%; (d) simulated stiffness degradation at 65%

4. Conclusion and future work

This paper investigated the characteristics of fatigue accumulation in CNFs modified resin embedded test coupons fabricated by PolyJet printing and comparisons to baseline digital PP material test coupons. This paper considered empirical fatigue modeling of experimental data. The simulated model was developed to predict the fatigue life of baseline, and CNF-resin embedded test coupons using modified 3D test coupon configurations of PolyJet printed simulated PP. For fatigue life prediction, it is essential to be able to precisely simulate the cumulative damage of PolyJet printed specimens. A linear function was evaluated to represent the S-N diagram. It was observed that there is a good correlation between the experimental life cycle. It predicted life cycle behavior with correlation coefficient, $R^2 = 0.9971$ for baseline and 0.9885 for CNF-resins embedded test coupons.

An empirical model was developed for predicting the stiffness of baseline and CNFs modified resin embedded test coupons printed with digital PP from PolyJet printing. The obtained fatigue life prediction model estimates the fatigue life of baseline and CNF resin-embedded test coupons at specific applied stress levels and their extrapolation to other stress levels, reducing the need for extensive additional fatigue tests. These results help to provide insight into understanding the fatigue behavior of nanomaterial systems. The nanoparticle-dispersed regions were added in tailored regions of the base components. The CNFs embedded test coupons show a lower average fatigue life and brittle

characteristic than the baseline digital PP. The lower fatigue life can be attributed to the initiation of stress or strain concentration that commonly degrades the mechanical properties since CNFs are stiffer than the polymer.

With this fatigue life and initial stiffness, the obtained empirical model can estimate the damage at any stage of the AM-printed simulated PP and be used to design AM parts for fatigue and cyclic loading. The empirical stiffness degradation model obtained is a polynomial of degree 4. The stiffness degradation model can thus be used to estimate the stiffness degradation. Results indicated that the fourth-order polynomial accurately predicts the stiffness degradation of simulated PP in PolyJet printing at any percentage of tension-tension fatigue stress levels, without requiring extensive testing.

With these conclusions in mind, the designer could potentially focus on tailoring materials in AM such that failure occurs in a specific location to maximize the fatigue life. This work showed significant data relating tailor material distribution of nanomaterials to fatigue life. In this paper, the authors seek to fill the gap in the literature by characterizing the fatigue life of a nano-modified materials system printed via PolyJet printing. In order to expand the breadth of this work, additional experimentation can be conducted in the future to:

• Assess the locations of voids to be filled with nano-materials;
• Analyze the fatigue life of specimens with varied shapes and sizes of the void to be filled with nanomaterials;
• Study the effect of the interface;
• Further optimizing the weight percentage of CNFs to reduce the stress concentration and maximize the fatigue life.

Conflict of interest

The authors declare that they have no conflict of interest.

References

[1] Tamez MBA, Taha I. A review of additive manufacturing technologies and markets for thermosetting resins and their potential for carbon fiber integration. *Additive Manufacturing*. 2021; 37: 101748. https://doi.org/10.1016/j.addma.2020.101748

[2] Najmon JC, Raeisi S, Tovar A. Review of additive manufacturing technologies and applications in the aerospace industry. In: Froes F, Boyer R. (eds.) *Additive manufacturing for the aerospace industry*. Amsterdam, Netherlands: Elsevier; 2019. p.7-31. https://doi.org/10.1016/B978-0-12-814062-8.00002-9

[3] Jiménez M, Romero L, Domínguez IA, Espinosa MDM, Domínguez M. Additive manufacturing technologies: An overview about 3D printing methods and future prospects. *Complexity*. 2019; 2019: 9656938. https://doi.org/10.1155/2019/9656938

[4] Tomar RPS, Ulu FI, Kelkar A, Mohan RV. Stiffness degradation of digital polypropylene under fatigue loading: Investigations via 3-dimensional Polyjet printed coupons. In: *Proceedings of the ASME 2020 International Mechanical Engineering Congress and Exposition. Volume 3: Advanced Materials: Design, Processing, Characterization, and Applications*. New York, United States: American Society of Mechanical Engineers; 2020. V003T03A005. https://doi.org/10.1115/imece2020-24156

[5] Degrieck J, Van Paepegem W. Fatigue damage modeling of fibre-reinforced composite materials: Review. *Applied Mechanics Reviews*. 2001; 54(4): 279-300. https://doi.org/10.1115/1.1381395

[6] Zhang Y, Vassilopoulos AP, Keller T. Stiffness degradation and fatigue life prediction of adhesively-bonded joints for fiber-reinforced polymer composites. *International Journal of Fatigue*. 2008; 30(10-11): 1813-1820. https://doi.org/10.1016/j.ijfatigue.2008.02.007

[7] Rotem A, Nelson HG. Failure of a laminated composite under tension-compression fatigue loading. *Composites Science and Technology*. 1989; 36(1): 45-62. https://doi.org/10.1016/0266-3538(89)90015-8

[8] Asp LE, Sjögren A, Greenhalgh ES. Delamination growth and thresholds in a carbon/epoxy composite under fatigue loading. *Journal of Composites, Technology and Research*. 2001; 23(2): 55-68. https://doi.org/10.1520/ctr10914j

[9] Tate JS, Kelkar AD. Stiffness degradation model for biaxial braided composites under fatigue loading. *Composites Part B: Engineering*. 2008; 39(3): 548-555. https://doi.org/10.1016/j.compositesb.2007.03.001

[10] Pertuz-Comas AD, Díaz JG, Meneses-Duran OJ, Niño-Álvarez NY, León-Becerra J. Flexural fatigue in a polymer

matrix composite material reinforced with continuous kevlar fibers fabricated by additive manufacturing. *Polymers*. 2022; 14(17): 3586. https://doi.org/10.3390/polym14173586
[11] Ulu FI, Mohan R, Tomar RPS. Development of thermally conductive Polymer/CNF nanocomposite materials via Polyjet additive manufacturing by improvement of digital material design. In: *Proceedings of the ASME 2019 International Mechanical Engineering Congress and Exposition. Volume 12: Advanced Materials: Design, Processing, Characterization, and Applications*. New York, United States: American Society of Mechanical Engineers; 2019. V012T10A059. https://doi.org/10.1115/imece2019-11556
[12] Tomar RPS, Ulu F, Mohan RV, Kelkar AD. Process induced variations in Polyjet printing under tension-tension fatigue loading – investigations via homogenous 3-dimensional test coupons. In: *SAMPE 2020 Virtual Conference*. The Society of the Advancement of Material and Process Engineering; 2020. http://dx.doi.org/10.33599/s.20.0234
[13] Ulu F, Tomar RPS, Mohan R. Processing and mechanical behavior of rigid and flexible material composite systems formed via voxel digital design in Polyjet additive manufacturing. *Rapid Prototyping Journal*. 2021; 27: 617-626. https://doi.org/10.1108/rpj-06-2020-0119
[14] Yuan S, Shen F, Chua CK, Zhou K. Polymeric composites for powder-based additive manufacturing: Materials and applications. *Progress in Polymer Science*. 2019; 91: 141-168. https://doi.org/10.1016/j.progpolymsci.2018.11.001
[15] Palanisamy C, Raman R, Dhanraj KP. Additive manufacturing: A review on mechanical properties of Polyjet and FDM printed parts. *Polymer Bulletin*. 2022; 79(9): 7065-7116. https://doi.org/10.1007/s00289-021-03899-0
[16] Dizon JRC, Espera Jr AH, Chen Q, Advincula RC. Mechanical characterization of 3D-printed polymers. *Additive Manufacturing*. 2018; 20: 44-67. https://doi.org/10.1016/j.addma.2017.12.002
[17] Doubrovski EL, Tsai EY, Dikovsky D, Geraedts JMP, Herr H, Oxman N. Voxel-based fabrication through material property mapping: A design method for bitmap printing. *Computer-Aided Design*. 2015; 60: 3-13. https://doi.org/10.1016/j.cad.2014.05.010
[18] Kawasaki A, Watanabe R. Concept and P/M fabrication of functionally gradient materials. *Ceramics International*. 1997; 23(1): 73-83. https://doi.org/10.1016/0272-8842(95)00143-3
[19] Moore JP, Williams CB. Fatigue properties of parts printed by PolyJet material jetting. *Rapid Prototyping Journal*. 2015; 21: 675-685. https://doi.org/10.1108/rpj-03-2014-0031
[20] Moore JP, Williams CB. Fatigue characterization of 3D printed elastomer material. In: *2012 International Solid Freeform Fabrication Symposium*. Austin, United States: University of Texas; 2012. p.641-655. http://dx.doi.org/10.26153/tsw/15379
[21] Kaweesa DV, Spillane DR, Meisel NA. Investigating the impact of functionally graded materials on fatigue life of material jetted specimens. In: *2017 International Solid Freeform Fabrication Symposium*. Austin, United States: University of Texas; 2017. p.578-592. https://hdl.handle.net/2152/89865
[22] Suresh JA, Kumar GS, Ramu P, Rengaswamy J. Fatigue life characterization of additively manufactured acrylic like Poly-Jet printed parts. In: Prakash R, Jayaram V, Saxena A. (eds.) *Advances in structural integrity.* Singapore: Springer; 2017. p.623-632. https://doi.org/10.1007/978-981-10-7197-3_52
[23] Bass LB, Meisel NA, Williams CB. Exploring variability in material properties of multi-material jetting parts. In: *2015 International Solid Freeform Fabrication Symposium*. Austin, United States: University of Texas; 2015. p.993-1006. https://hdl.handle.net/2152/89395
[24] Kęsy A, Kotliński J. Mechanical properties of parts produced by using polymer jetting technology. *Archives of Civil and Mechanical Engineering*. 2010; 10(3): 37-50. https://doi.org/10.1016/s1644-9665(12)60135-6
[25] Gay P, Blanco D, Pelayo F, Noriega A, Fernández P. Analysis of factors influencing the mechanical properties of flat PolyJet manufactured parts. *Procedia Engineering*. 2015; 132: 70-77. https://doi.org/10.1016/j.proeng.2015.12.481
[26] Barclift MW, Williams CB. Examining variability in the mechanical properties of parts manufactured via Polyjet direct 3D printing. In: *2012 International Solid Freeform Fabrication Symposium*. Austin, United States: University of Texas; 2012. p.876-890. http://dx.doi.org/10.26153/tsw/15397
[27] Tomar RPS, Ulu FI, Kelkar A, Mohan RV. Investigation of process induced variations in PolyJet printing with digital polypropylene via homogeneous 3D tensile test coupon. In: *Proceedings of the ASME International Mechanical Engineering Congress and Exposition. Volume 12: Advanced Materials: Design, Processing, Characterization, and Applications*. New York, United States: American Society of Mechanical Engineers; 2019. V012T10A060. https://doi.org/10.1115/imece2019-11639
[28] Mao H, Mahadevan S. Fatigue damage modelling of composite materials. *Composite Structures*. 2002; 58(4): 405-410. https://doi.org/10.1016/s0263-8223(02)00126-5
[29] Tomar RPS, Ulu F, Mohan DR, Kelkar A. Investigation of process variation effects via a homogeneous 3-dimensional tensile test coupon in Polyjet 3D additive printing. In: *SAMPE 2019*. Charlotte, United States: The Society of the Advancement of Material and Process Engineering; 2019. https://doi.org/10.33599/nasampe/

s.19.1546
[30] Martin DE, Severns AE, Kabo JM. Determination of mechanical stiffness of bone by pQCT measurements: Correlation with non-destructive mechanical four-point bending test data. *Journal of Biomechanics.* 2004; 37(8): 1289-1293. https://doi.org/10.1016/j.jbiomech.2003.12.009
[31] McMeeking R, Evans A. Matrix fatigue cracking in fiber composites. *Mechanics of Materials*. 1990; 9(3): 217-227. https://doi.org/10.1016/0167-6636(90)90004-y
[32] Van Paepegem W, Degrieck J. A new coupled approach of residual stiffness and strength for fatigue of fibre-reinforced composites. *International Journal of Fatigue*. 2002; 24(7): 747-762. https://doi.org/10.1016/S0142-1123(01)00194-3